







ORIGINAL ARTICLE

KLK10 derived from tumor endothelial cells accelerates colon cancer cell proliferation and hematogenous liver metastasis formation

Kazuya Kato | Takehiro Noda  | Shogo Kobayashi  | Kazuki Sasaki |
 Yoshifumi Iwagami | Daisaku Yamada  | Yoshito Tomimaru  | Hidenori Takahashi  |
 Mamoru Uemura | Tadafumi Asaoka | Junzo Shimizu | Yuichiro Doki |
 Hidetoshi Eguchi 

Department of Gastroenterological Surgery, Graduate School of Medicine, Osaka University, Osaka, Japan

Correspondence

Shogo Kobayashi, Department of Gastroenterological Surgery, Graduate School of Medicine, Osaka University, 2-2 (E2), Yamadaoka, Suita, Osaka 565-0871, Japan.

Email: s-kobayashi@umin.ac.jp

Funding information

Japan Society for the Promotion of Science, Grant/Award Number: (C) 22K08870 and (C) 22K16530

Abstract

Tumor endothelial cells (TECs), which are thought to be structurally and functionally different from normal endothelial cells (NECs), are increasingly attracting attention as a therapeutic target in hypervascular malignancies. Although colorectal liver metastasis (CRLM) tumors are hypovascular, inhibitors of angiogenesis are a key drug in multidisciplinary therapy, and TECs might be involved in the development and progression of cancer. Here, we analyzed the function of TEC in the CRLM tumor microenvironment. We used a murine colon cancer cell line (CT26) and isolated TECs from CRLM tumors. TECs showed higher proliferation and migration than NECs. Coinjection of CT26 and TECs yielded rapid tumor formation *in vivo*. Immunofluorescence analysis showed that coinjection of CT26 and TECs increased vessel formation and Ki-67⁺ cells. Transcriptome analysis identified kallikrein-related peptide 10 (KLK10) as a candidate target. Coinjection of CT26 and TECs after KLK10 downregulation with siRNA suppressed tumor formation *in vivo*. TEC secretion of KLK10 decreased after KLK10 downregulation, and conditioned medium after KLK10 knockdown in TECs suppressed CT26 proliferative activity. Double immunofluorescence staining of KLK10 and CD31 in CRLM tissues revealed a significant correlation between poor prognosis and positive KLK10 expression in TECs and tumor cells. On multivariate analysis, KLK10 expression was an independent prognostic factor in disease-free survival. In conclusion, KLK10 derived from TECs accelerates colon cancer cell proliferation and hematogenous liver metastasis formation. KLK10 in TECs might offer a promising therapeutic target in CRLM.

KEYWORDS

hepatectomy, hypovascular tumor, metastatic liver cancer, prognosis, tumorigenesis

Abbreviations: CA19-9, carbohydrate antigen 19-9; CEA, carcinoembryonic antigen; CM, conditioned medium; CRC, colorectal cancer; CRLM, colorectal liver metastasis; CT26, CT26. WT murine colon carcinoma cell line; DFS, disease-free survival; HCC, hepatocellular carcinoma; KLK10, kallikrein-related peptide 10; NEC, normal endothelial cell; NGS, next-generation sequencing; OS, overall survival; TC, tumor cell; TEC, tumor endothelial cell.

This is an open access article under the terms of the [Creative Commons Attribution-NonCommercial](https://creativecommons.org/licenses/by-nc/4.0/) License, which permits use, distribution and reproduction in any medium, provided the original work is properly cited and is not used for commercial purposes.

© 2024 The Authors. *Cancer Science* published by John Wiley & Sons Australia, Ltd on behalf of Japanese Cancer Association.

1 | INTRODUCTION

Colorectal cancer (CRC) is the third most common cancer, diagnosed in about 1.9 million people each year worldwide, with increasing incidence rates in many countries.¹ CRC has a high rate of hematogenous distant metastasis, the liver being the commonest site.² Hepatectomy and chemotherapy are the standard treatment in patients with resectable or unresectable colorectal liver metastasis (CRLM). Chemotherapy with antivascular endothelial growth factor monoclonal antibodies is one of the standardized regimens and has led to improved prognosis.³⁻⁵ Despite recent advances in treatment, more than 70% of patients experience recurrence after curative resection,^{6,7} so the therapeutic outcome of CRLM remains unsatisfactory.

In many cancers, distant metastasis is one of the poor prognostic factors. Tumor blood vessels play an important role in hematogenous metastasis of cancer cells.^{8,9} The characteristics and functions of tumor endothelial cells (TECs) differ in many respects from normal endothelial cells (NECs). Tumor blood vessels have sparse pericyte binding and fragile adhesion between TECs, making it easier for cancer cells to enter the vessels and promoting metastasis.¹⁰ TECs are also reported to interact with tumor cells (TCs) and affect tumor growth, metastasis, and immunosuppression of the tumor microenvironment.¹¹⁻¹⁴ The normalization of tumor vessels in terms of their structure and function is predicted to improve tumor blood perfusion and result in reduced tumor metastasis.^{10,14,15} As these reports indicate, TECs are once again attracting attention as a therapeutic target for cancer.

Many studies on TECs have been conducted on hypervascularized tumors such as hepatocellular carcinoma (HCC), renal carcinoma, and lung cancer.¹⁶⁻¹⁸ In a hypovascular tumor such as CRLM, the interaction between TCs and TECs has not yet been studied. However, in the clinical setting, inhibitors of angiogenesis are now widely used for treating CRLM in multidisciplinary therapy.^{19,20} To overcome the high recurrence rate and unsatisfactory outcomes in CRLM, a new treatment strategy of targeting TECs is very promising.

In this study, we investigated the influence of TECs on CRLM tumor growth *in vitro* and *in vivo*, with focus on the interaction between TECs and TCs. We performed next-generation sequencing (NGS) on TECs and NECs to identify potential treatment targets and pinpointed kallikrein-related peptide 10 (KLK10) as a candidate. Finally, we investigated the effects and mechanisms related to KLK10 as a target in TECs.

2 | MATERIALS AND METHODS

2.1 | Drugs and reagents

Bovine serum albumin was obtained from Sigma-Aldrich, and ProLong Glass Antifade Mountant with NucBlue™ Stain from

Thermo Fisher Scientific. Mouse recombinant KLK10 Protein was purchased from Abxexa (abx651828).

2.2 | Cell line and culture conditions

The CT26.WT (CRL-2638) murine colon carcinoma cell line (CT26) and BNL 1 ME A.7R.1 murine HCC cell line (BNL) were purchased from ATCC. Colon26 was purchased from RIKEN BioResource Research Center. These cells were maintained in low-glucose DMEM (Nacalai Tesque) supplemented with 10% FBS (Invitrogen) and cultivated in a humidified incubator at 37°C under 5% CO₂.

2.3 | Animal experiments

Animal experiments were conducted using male BALB/cAJcl-nu/nu immunodeficient mice and BALB/cAJcl immunocompetent mice aged 6–10 weeks (CLEA Japan). For isolation of TECs, we injected 5×10^5 CT26 cells and colon26 cells into the spleen of BALB/cAJcl-nu/nu mice to create the CRLM tumor model. We harvested CRLM tumors or healthy livers from BALB/cAJcl-nu/nu mice and isolated endothelial cells as previously reported.¹⁶ Isolated CD31⁺ cells were plated and grown in Endothelial Cell Growth Medium 2-MV (Lonza) in a humidified incubator.

For the HCC tumor model, we injected the spleens of BALB/cAJcl mice with 20×10^4 BNL cells. For the subcutaneous tumor model, we injected BALB/cAJcl mice subcutaneously with 50×10^4 CT26 cells (CT26 group), 45×10^4 CT26 cells + 5×10^4 NECs (CT26 + NEC group), or 45×10^4 CT26 cells + 5×10^4 TECs (CT26 + TEC group) ($n=4$ per group). For the CRLM tumor model, we injected the spleens of BALB/cAJcl mice with 20×10^4 CT26 cells (CT26 group), 18×10^4 CT26 cells + 2×10^4 NECs (CT26 + NEC group), or 18×10^4 CT26 cells + 2×10^4 TECs (CT26 + TEC group) ($n=4$ per group). Body weight progress and resected liver weights were compared. All mouse tumor models had their tumors harvested after 2 weeks.

2.4 | Flow cytometry

Tumor endothelial cells and normal endothelial cells were detached with trypsin-EDTA. Then, these cells were incubated with anti-CD105 antibodies (BioLegend) and analyzed using a FACS Calibur flow cytometer (Novocyte Quanteon, Agilent) and FACS Diva™ software (NovoExpress, Agilent).

2.5 | In vitro functional assays

Tube formation was analyzed as previously described.²¹ In a proliferation assay, endothelial cells or TCs were assessed using the

CCK-8 assay (Dojindo).²² CT26 cells were treated with mouse recombinant KLK10 protein (10 ng/mL) or conditioned medium (CM) of TECs transfected with siRNA, and proliferation rates were investigated. In the migration assay, NECs and TECs were evaluated using the scratch assay.²³ Wound closure was expressed as the ratio of the percentages of wound-closing areas, measured in high-power fields.

2.6 | Western blotting

Western blot analysis was performed as previously described.²⁴ The primary antibodies were anti-CD31 (Abcam), anti-KLK10 (Invitrogen), and anti- β -actin (Sigma-Aldrich).

2.7 | Immunocytochemical staining

Immunocytochemistry was performed as previously described.²⁵ Briefly, cells were stained with anti-CD31 antibody (Abcam). After being counterstained with DAPI, slides were evaluated under a fluorescence microscope (BZ-X700; Keyence).

2.8 | Immunofluorescence analysis

All immunostaining methods have been previously described.^{16,26} Immunostaining was performed with the following primary antibodies: anti-KLK10 (Invitrogen), anti-CD31 (Abcam), and anti-Ki-67 (Abcam). TC proliferation was assessed as the percentage of Ki-67⁺ nuclei from the total number of nuclei. The images were observed using a BZ-X700 microscope and independently evaluated by two investigators using BZ-X Analyzer software (Keyence).

2.9 | RNA sequencing and data analysis

RNA sequencing and data analysis were performed as previously described.²⁷ We excluded mRNAs that were undetectable. Candidate target mRNAs were defined as those showing more than a 64-fold difference between NEC and TEC expression levels or fourfold difference between TEC scramble siRNA and TEC KLK10 siRNA-1/-2.

2.10 | Quantitative RT-PCR

Quantitative RT-PCR (qRT-PCR) was performed as previously described.²⁸ The following primers were used: KLK10, 5'-GGCCAGTATCGACGAGAGG-3' (forward) and 5'-CAAAAACCGCAACATGACCTTC-3' (reverse); and GAPDH, 5'-CCAACCGCGAGAAATGACC-3' (forward) and 5'-GGAGTCCATCACGATGCCAG-3' (reverse).

2.11 | siRNA

KLK10 expression in TECs and CT26 cells was downregulated by siRNA method as previously described.^{25,27} As a control, these cells were transfected with Scrambled siRNA (Life Technologies). Transfected cells were analyzed with a proliferation assay and wound-healing assay. The in vivo effect of TECs transfected with KLK10-siRNA on tumorigenesis also was tested. Briefly, 45×10^4 CT26 cells + 5×10^4 transfected TECs (Scramble siRNA, KLK10 siRNA-1, and KLK10 siRNA-2) were injected subcutaneously and 18×10^4 CT26 cells + 2×10^4 transfected TECs were injected into the spleen in each mouse ($n=4$ per group). Tumor volume, body weight, and liver weight were compared.

2.12 | ELISA

KLK10 secreted into the CM from TECs was measured by using a mouse KLK10 ELISA kit (MyBioSource, MBS035638) according to the manufacturer's protocol. The culture supernatants of transfected TECs (Scramble siRNA, KLK10 siRNA-1, and KLK10 siRNA-2) were collected and centrifuged at $1000 \times g$ for 20 min.

2.13 | Patients and tissue samples

Immunofluorescence analysis was performed using samples from 77 consecutive patients who underwent curative surgery for CRLM from January 2010 to December 2018 at the Department of Gastroenterological Surgery at Osaka University Hospital. Histological classification was determined according to the Japanese Classification.²⁹ TECs were defined as CD31⁺ cells in the tumor lesion. KLK10⁺ TECs were counted as the number of CD31⁺ KLK10⁺ nuclei and analyzed as a percentage of the total number of CD31⁺ nuclei. KLK10⁺ TCs were counted as the number of CD31⁻ KLK10⁺ nuclei and analyzed as a percentage of the total number of CD31⁻ nuclei. For each measurement, samples were divided based on positive ($\geq 1\%$) versus negative expression ($< 1\%$).

2.14 | Statistical analysis

The patients' clinicopathological indicators were compared using Chi-squared tests and Student's *t*-tests. Continuous variables were compared using Mann-Whitney's *U*-tests or Student's *t*-tests. Survival curves were analyzed using the Kaplan-Meier method, and differences were compared by the log-rank test. To evaluate the risks associated with the prognostic variables, univariate and multivariate analyses using a Cox model were performed with determination of the hazard ratio and 95% confidence interval. Statistical analyses were performed using R version 4.2.2 (Vienna, Austria; <http://www.R-project.org/>). A $p < 0.05$ was considered to be statistically significant.

3 | RESULTS

3.1 | Tumor endothelial cell and normal endothelial cell isolation and in vitro assay

We isolated TECs from CRLM tumors and NECs from normal liver. The schema of experiments is shown in [Figure 1A](#). In the purity of TECs and NECs, more than 95% of isolated TECs and NECs showed positive expression of CD105 that were specific markers for endothelial cells ([Figure S1A](#)). On immunocytochemistry, both TECs and NECs showed significantly higher expression levels of CD31 compared with CT26 cells ([Figure 1B](#)). In the tube formation assay, TECs and NECs formed round tubes characteristic of cultured endothelial cells, whereas CT26 cells did not show tube formation ([Figure 1C](#)). Western blotting confirmed that CD31 protein expression also was significantly higher in TECs and NECs ([Figure 1D](#)). These results suggest that TECs and NECs could be successfully isolated from tumors and maintain their endothelial cell characteristics after cell isolation. To examine the validity of the CT26 and colon26 tumor model as hypovascular tumor, the vascularity of the CRLM tumor of CT26 and colon26 was compared with the hypovascular tumor, the HCC tumor of BNL cells. The CRLM tumor of CT26 and colon26 showed about 42%–24% of structured tumor vessels of the HCC tumor of BNL (15.4, 8.6, and 36.4/field, respectively; $p < 0.001$, [Figure S1B](#)). TECs could only be isolated from the CRLM tumor of CT26 cells. Sufficient TECs could not be obtained from the CRLM tumors of colon26 cells, which had fewer vessels than the tumor of CT26 cells, and future studies were performed with TECs isolated from tumors of CT26 cells. In the functional wound-healing ([Figure 1E](#)) and proliferation assays ([Figure 1F](#)), compared with NECs, TECs showed greater migratory activity (62.4% vs. 22.4%, $p < 0.001$) and proliferative capacity ($p = 0.001$).

3.2 | In vivo analysis of TEC and NEC tumorigenesis

The schema of in vivo experiments is shown in [Figure 2A](#). In the subcutaneous tumor model, the CT26+TEC group showed more rapid tumor formation than the other two groups (CT26 and CT26+NEC groups) ([Figure 2B](#)). The subcutaneous tumor of the CT26+TEC group showed significantly more vessels (31.6/field) than the CT26 group and CT26+NEC group (11.8 and 20.2/field, respectively; $p < 0.001$; [Figure 2C](#)). [Figure 2D](#) shows the appearance of harvested CRLM tumors 2 weeks after splenic injection of each group. Body weight progress did not differ significantly among the three groups ($p = 0.532$; [Figure 2E](#)), but liver weights were significantly greater in the CT26+TEC group (6.1 g) than in the CT26 and CT26+NEC groups (2.1 and 2.3 g, respectively; $p < 0.001$; [Figure 2F](#)). The CT26+TEC

group showed significantly more vessels (56.0/field) than the CT26 and CT26+NEC groups (12.2 and 24.4/field, respectively; $p < 0.001$; [Figure 2G](#)). Ki-67⁺ cells were significantly more numerous in the CT26+TEC group (49.8%) than in the CT26 group and CT26+NEC group (25.0% and 34.2%; respectively; $p < 0.001$; [Figure 2H](#)).

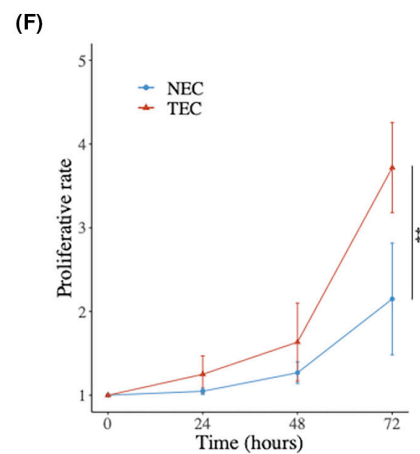
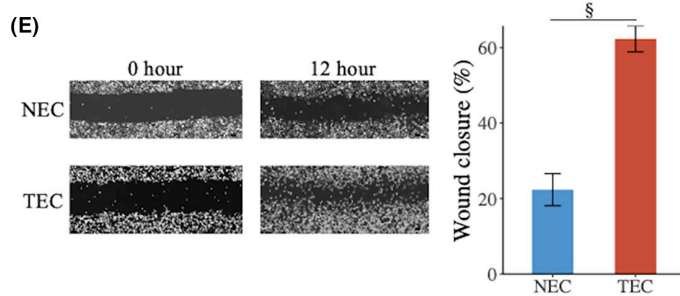
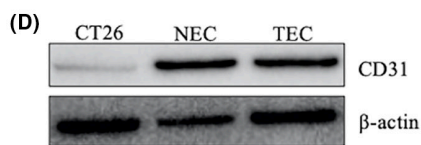
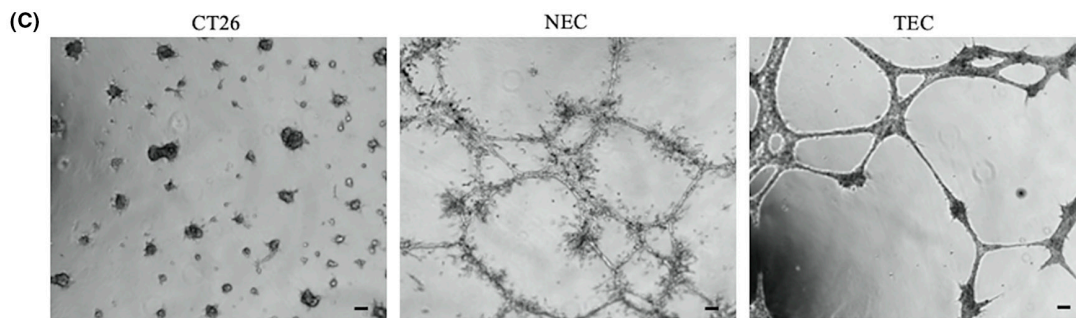
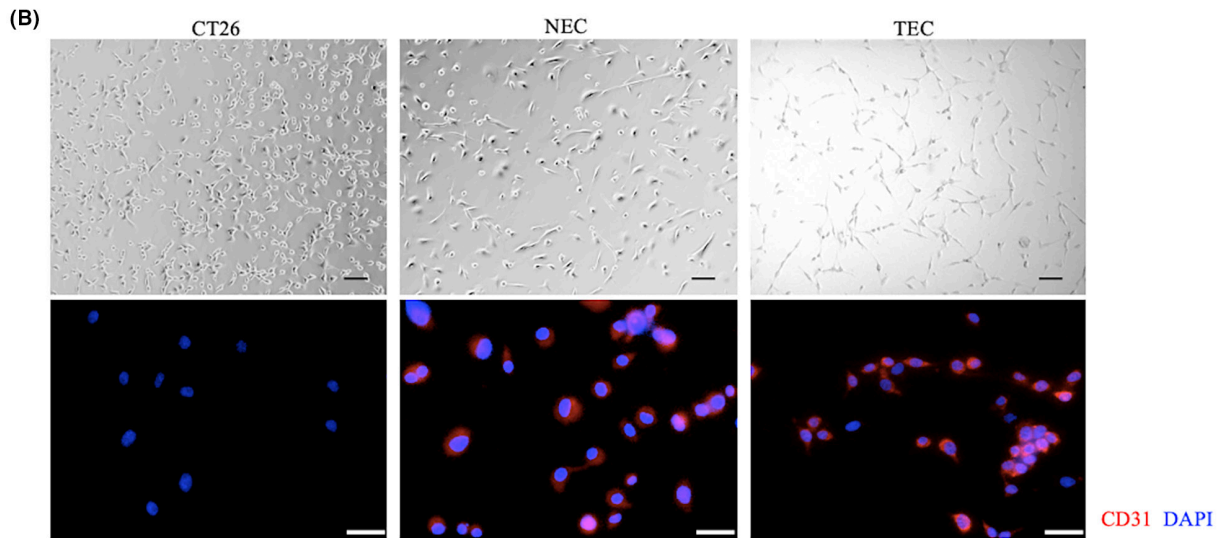
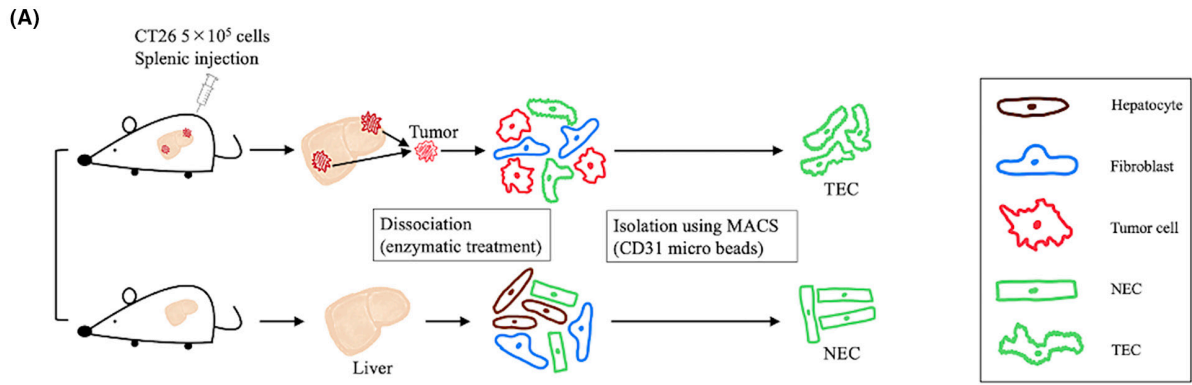
3.3 | Transcriptome analysis with NGS

We speculated that some factors secreted from TECs might accelerate the growth of CT26 cells and tumor formation in a subcutaneous tumor model and CRLM tumor model. Therefore, we performed a transcriptome analysis of NECs and TECs using NGS. The results yielded 127 mRNAs showing a more than 64-fold difference between NECs and TECs. The heatmap of 127 genes is shown in [Figure 3A](#), and [Table S1](#) shows the gene list. Of the 127 genes differentially expressed between TECs and NECs, we selected KLK10, which was highly expressed in TECs and had been previously reported to be associated with vascular endothelial cells and cell proliferation, for more detailed study. The KLK10 mRNA expression level in TECs was upregulated compared with NECs and CT26 cells ([Figure 3B](#)), and Western blotting confirmed increased KLK10 protein expression in TECs, as well ([Figure 3C](#)).

3.4 | Downregulation of KLK10 expression in TECs and CT26 cells

After downregulation of KLK10 by siRNA (KLK10 siRNA-1 and KLK10 siRNA-2), KLK10 expression was significantly suppressed to approximately 10% of that in TECs transfected with Scramble siRNA ([Figure 3D](#)). Western blotting confirmed that KLK10 protein expression was also suppressed ([Figure 3E](#)). Immunocytochemistry of CD31 for Klk10 siRNA-transfected TECs demonstrated that the CD31 expression was maintained in TEC Scramble siRNA, TEC KLK10 siRNA-1, and TEC KLK10 siRNA-2 ([Figure S2A](#)). The results of the wound-healing assay showed that downregulation of KLK10 in TECs decreased their migratory ability ([Figure 3F](#)). The wound closure ratio was 18.4% in cells transfected with KLK10 siRNA-1, 24.1% in cells transfected with KLK10 siRNA-2, and 46.0% in cells transfected with Scramble siRNA ($p < 0.001$). The proliferation assay also showed that downregulation of KLK10 in TECs resulted in decreased TEC proliferation ($p < 0.001$; [Figure 3G](#)). In addition, we performed a transcriptome analysis after knockdown of KLK10 in TECs to investigate the molecular mechanisms of the downstream of KLK10. The results yielded 148 mRNAs showing a more than fourfold difference between TEC scramble siRNA and TEC KLK10 siRNA-1/-2 ([Table S2](#)). For CT26 cells, a slight decrease in KLK10 protein expression was observed after

FIGURE 1 Isolation of TECs and NECs and comparison of their characteristics. (A) Schematic showing isolation method of TECs and NECs. (B) Morphological analysis (scale bars: 100 μ m) and immunocytochemistry analysis (scale bars: 50 μ m). (C) Tube formation assay (scale bars: 100 μ m). (D) Western blotting. (E) Wound-healing assay (left; scale bars: 100 μ m) and quantification of the wound closure rate (right). (F) Proliferation assay. [†] $p < 0.005$; [§] $p < 0.001$. TEC, tumor endothelial cell; NEC, normal endothelial cell.



downregulating KLK10 by siRNA (Figure S2B). And, the downregulation of KLK10 expression in CT26 cells resulted in a slight decrease in proliferative ability of CT26 cells ($p=0.014$; Figure S2C).

3.5 | Downregulation of KLK10 expression in TECs and inhibited tumor formation in vivo

The effect of KLK10 downregulation in TECs was examined in vivo. The schema of this experiment is shown in Figure 4A. In the subcutaneous tumor model, the CT26+TEC KLK10 siRNA-1 group and the CT26+TEC KLK10 siRNA-2 group suppressed tumor formation compared with the CT26+TEC Scramble siRNA group ($p=0.001$; Figure 4B). CD31 immunofluorescence analysis showed that the CT26+TEC KLK10 siRNA-1 group and the CT26+TEC KLK10 siRNA-2 group had significantly fewer vessels than the CT26+TEC Scramble siRNA group (19.8 and 17.6/field vs. 31.4/field, respectively; $p<0.001$; Figure 4C). Figure 4D shows the appearance of harvested CRLM tumors 2 weeks after splenic injection of each group. In the CRLM tumor model, body weight progress did not differ significantly among the three groups ($p=0.704$; Figure 4E), but liver weights were significantly lighter in the CT26+TEC KLK10 siRNA-1 group and the CT26+TEC KLK10 siRNA-2 group (3.4 g and 3.5 g, respectively) than in the CT26+TEC Scramble siRNA group (4.8 g; $p=0.024$; Figure 4F). The immunofluorescence staining of CD31 showed that the number of vessels was significantly lower in the CT26+TEC KLK10 siRNA-1 group and the CT26+TEC KLK10 siRNA-2 group (33.4 and 32.2/field, respectively) than in the CT26+TEC Scramble siRNA group (62.4/field; $p<0.001$). The double-immunofluorescence staining of CD31 and KLK10 showed that the ratio of KLK10-positive vessels to total vessels was kept as under 20% level of the control through the experiment (80.4% in the CT26+TEC Scramble siRNA group, 14.1% in the CT26+TEC KLK10 siRNA-1 group, and 13.3% in the CT26+TEC KLK10 siRNA-2 group; $p<0.001$; Figure 4G). Moreover, immunofluorescence Ki-67 staining showed a significantly decreased ratio of Ki-67⁺ cells in the CT26+TEC KLK10 siRNA-1 group (38.1%) and the CT26+TEC KLK10 siRNA-2 group (35.3%) compared with the CT26+TEC Scramble siRNA group (48.2%; $p<0.001$; Figure 4H).

3.6 | KLK10 secretion and culture of cancer cells with CM after KLK10 knockdown in TECs

The amount of KLK10 secreted from TECs was significantly decreased when KLK10 expression in TECs was suppressed (Scramble

siRNA: 2393 pg/mL; KLK10 siRNA-1: 744 pg/mL; and KLK10 siRNA-2: 669 pg/mL; $p<0.001$; Figure 5A). To investigate the effect of KLK10 secreted from TECs on cancer cell proliferation, we performed the experiment with CT26 cells treated with recombinant KLK10 protein. When CT26 cells were cultured in medium with KLK10, the proliferative ability of CT26 cells was increased by adding the recombinant KLK10 protein to the medium ($p<0.001$; Figure 5B). Moreover, the CM was obtained after transfection of TECs with Scramble siRNA, KLK10 siRNA-1, or KLK10 siRNA-2. CT26 cells were cultured with CM for 72 h after seeding and the proliferative activity of each cell assessed (see Figure 5C for experimental schema). The proliferative ability of CT26 cells cultured with CM of KLK10 siRNA-1 or siRNA-2 was significantly decreased compared with that using CM of Scramble siRNA ($p=0.005$; Figure 5D).

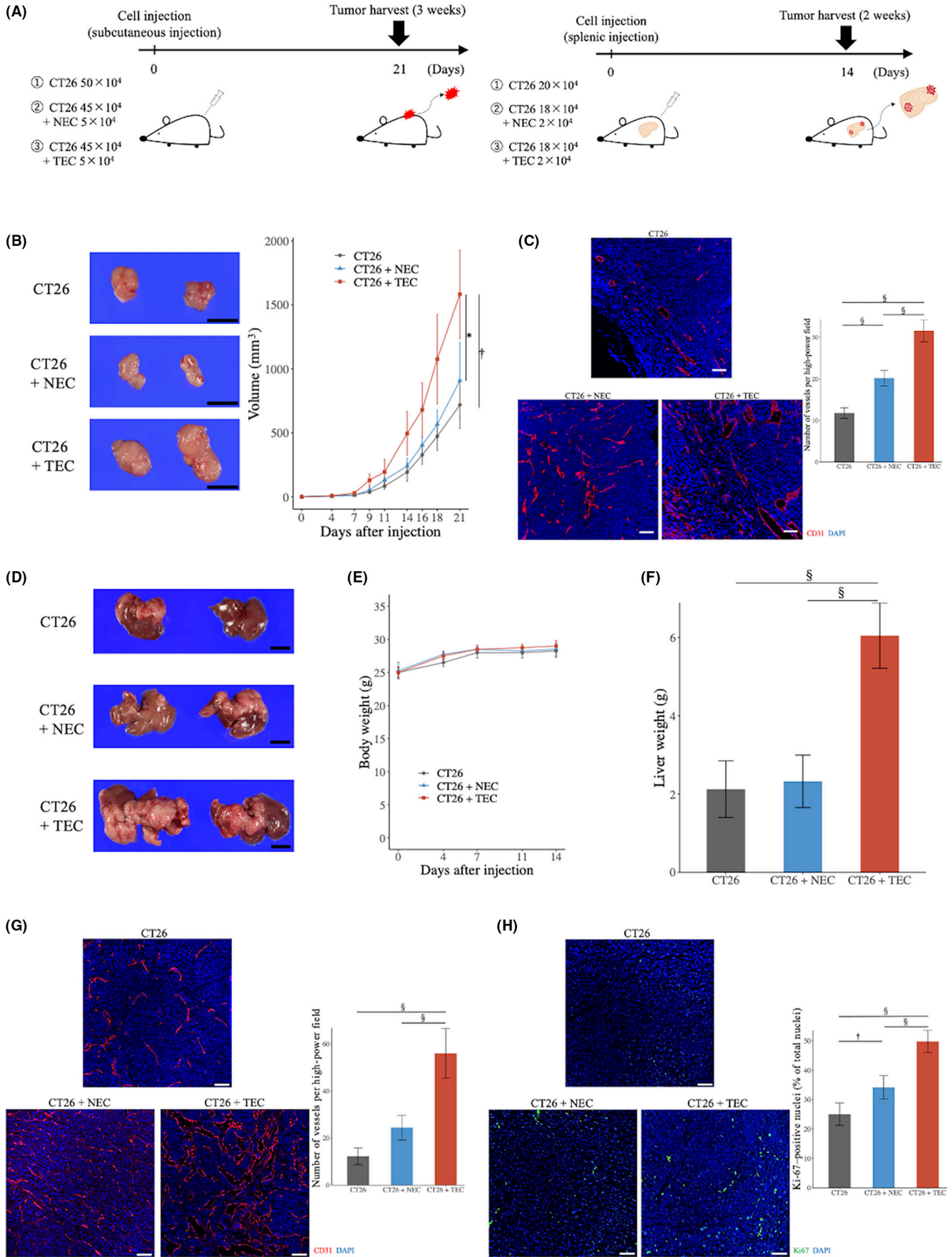
3.7 | KLK10 expression in TECs and TCs and survival

To investigate the clinical significance of KLK10 expression in patients with CRLM, we used immunofluorescence staining to examine KLK10 expression of resected liver specimens from patients. Table 1 summarizes their clinicopathological characteristics. In tumor lesions, positive expression of KLK10 in TECs was found in 49.4% of patients with CRLM (38/77 cases), and positive expression in TCs was found in 35.1% (27/77 cases; Figure 6A). Patients were divided into four groups based on KLK10 expression status in TECs and TCs: TEC⁺/TC⁺ ($n=20$), TEC⁺/TC⁻ ($n=18$), TEC⁻/TC⁺ ($n=7$), and TEC⁻/TC⁻ ($n=32$). Table 2 shows the results for the comparison of the clinicopathological factors between the TEC⁺/TC⁺ group ($n=20$) and the remaining patients ($n=57$), none of which were significant.

In all 77 patients, the median postoperative follow-up time was 4.37 years (0.08–12.24 years). The median recurrence-free survival time was 1.16 years (0.85–4.23 years). Figure 6B shows the disease-free survival (DFS) curves for the four groups. The TEC⁺/TC⁺ group had the worst DFS and overall survival (OS). In the comparison of survival curves between the TEC⁺/TC⁺ group and the other remaining patients (Figure 6C), the TEC⁺/TC⁺ group had significantly shorter DFS and OS rates than the others, with respective 2-year DFS rates of 15.9% and 49.8% ($p=0.001$) and 5-year OS rates of 40.1% and 69.5% ($p=0.007$).

Tables 3 and 4 show the results of univariate and multivariate analyses of DFS and OS. Multivariate analysis of DFS identified two independent significant factors: CA19-9 value ($p<0.001$) and positive expression of KLK10 in both TECs and TCs ($p=0.002$). In

FIGURE 2 Differences in tumorigenesis effects between NECs and TECs in vivo. (A) Schematic illustration of the experiment: subcutaneous tumor model (left) and CRLM tumor model (right). (B) Representative pictures of subcutaneous tumors (scale bars: 10 mm) and tumor volumes (right). (C) Immunofluorescence images of CD31 staining in subcutaneous tumor (scale bars: 50 μ m) and quantification of vessel numbers (right). (D) Representative pictures of CRLM tumors (scale bars: 10 mm). (E) Body weight progress. (F) Liver weight. (G) Immunofluorescence images of CD31 staining in CRLM tumor (scale bars: 50 μ m) and quantification of vessel numbers (right). (H) Immunofluorescence images of Ki-67 staining in CRLM tumor (scale bars: 50 μ m). Proportions of Ki-67⁺ cells among the total number of cells with intact nuclei (right). * $p<0.05$; † $p<0.01$; ‡ $p<0.001$. CRLM, colorectal liver metastasis; TEC, tumor endothelial cell; NEC, normal endothelial cell.



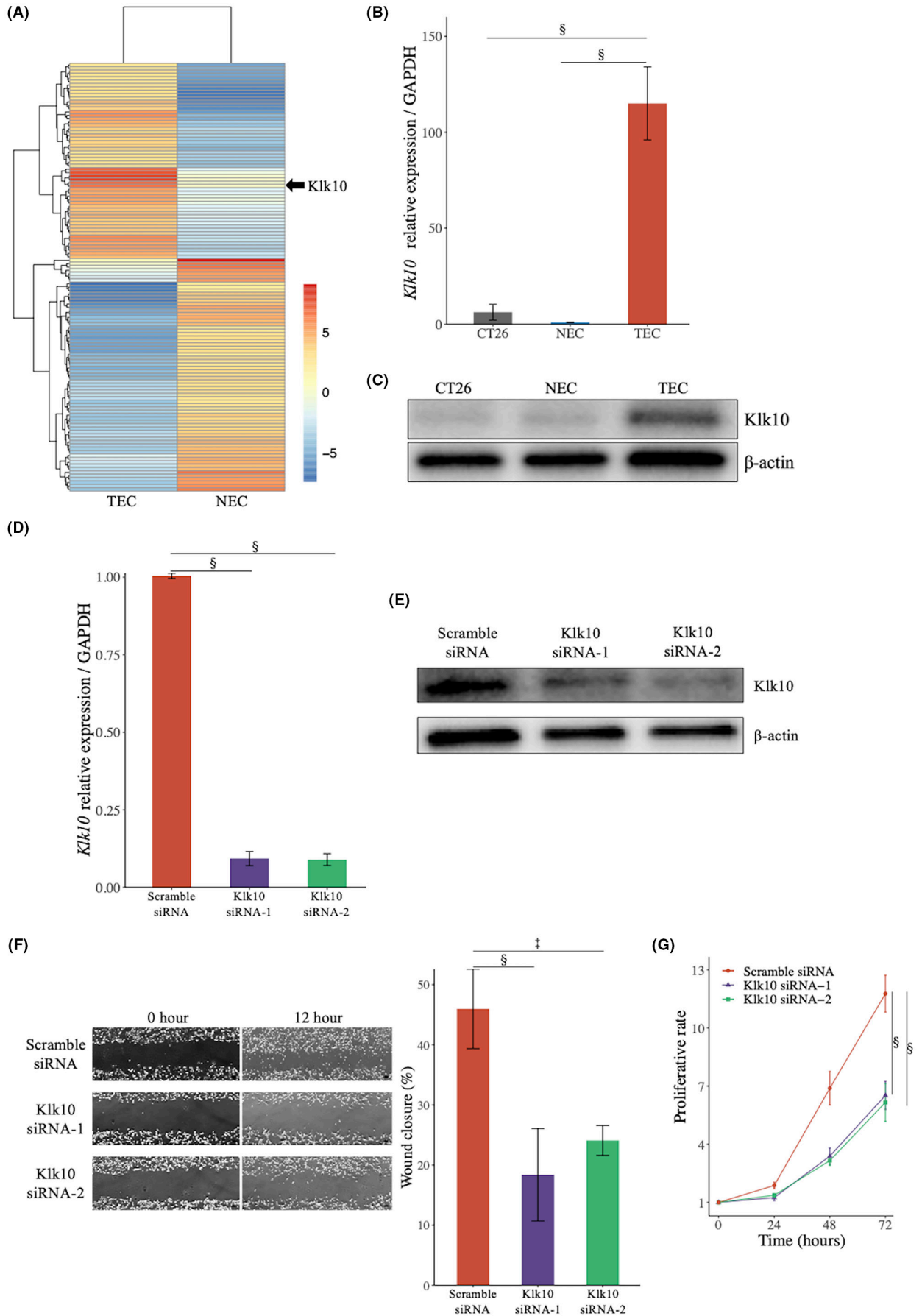


FIGURE 3 Comparison of mRNA expression levels between TECs and NECs by NGS. (A) Heatmap analysis. (B) qRT-PCR. (C) Western blotting. (D) qRT-PCR of siRNA-transfected TECs. (E) Western blotting of siRNA-transfected TECs. (F) TEC migration after downregulation of Klk10 expression (scale bars: 100 μ m). Quantification of the wound closure rate (right). (G) TEC proliferation after downregulation Klk10 expression. [‡] $p < 0.005$; [§] $p < 0.001$. NEC, normal endothelial cell; NGS, next-generation sequencing; TEC, tumor endothelial cell.

terms of OS, positive KLK10 expression in both TECs and TCs was a significant prognostic factor in univariate analysis ($p = 0.009$) but not in multivariate analysis, although there was a trend toward poor prognosis (hazard ratio = 2.05 [0.91–4.65], $p = 0.084$).

4 | DISCUSSION

In this study, we demonstrated that TECs promote tumor growth in CRLM and KLK10 in TECs might function as a novel therapeutic target. In fact, downregulation of KLK10 in TECs suppressed tumor growth in vivo, and immunofluorescence analysis of resected CRLM specimens revealed positive expression of KLK10 in both TECs and TCs as a poor prognostic factor.

Previous studies in hypervascularized tumors have shown that TECs (tumor vessels) have abnormality of structural, functional, and molecular characteristics, which contributes to tumor progression.^{13,18,30,31} However, our understanding of TECs in hypovascular tumors such as CRLM is insufficient. In our study, we performed a transcriptome analysis using NGS to reveal the aberrant molecular nature of TECs in CRLM and found high expression of KLK10. KLK10 is a secreted protein and member of the 15 kallikrein subfamily clustered at chromosome region 19q13.4.³² KLK10 has been found to be upregulated in many types of malignancies, including pancreatic ductal adenocarcinoma, ovarian cancer, and gastric cancer, and it is considered one of the potential markers of poor prognosis.^{33–35} It also has been reported that in vitro downregulation of KLK10 expression inhibits glycolytic metabolism and decreases cell viability, suggesting a relationship with the PI3K/Akt/mTOR pathway.³⁶ Furthermore, the expression of KLK10 by endothelial cells has been associated with regulation of vascular inflammation, such as atherosclerosis.³⁷ KLK10 expression in TECs has not previously been investigated, however.

In the current work, we demonstrated that coinjection of TECs and CT26 cells promotes TC growth, indicating interaction between TECs and TCs and some effect of TECs on the growth of cancer cells. Next, we found overexpression of KLK10 in TECs by RNA sequencing and that secreted KLK10 accelerated TC proliferation. These results suggest that KLK10 secreted from TECs may affect cancer cell proliferation by a paracrine mechanism. Previous reports have described coinjection of TECs and TCs as promoting tumorigenesis by several mechanisms. TECs secrete molecules such as bone morphogenetic proteins, fibroblast growth factors, and biglycan, which are well known to promote cancer cell growth and metastasis.^{38,39} We showed that TECs in CRLM secreted KLK10 that could promote TC growth and that inhibition of KLK10 expression in TECs could suppress cancer cell proliferation and metastatic tumor formation. We also performed experiments to investigate KLK10 expression

and its significance in TCs. However, KLK10 expression in CT26 cells tended to be much less than that in TECs, and downregulating KLK10 expression in CT26 cells had a slight and limited effect on proliferative ability. It is possible that human TCs secrete KLK10 and are involved in TC proliferation, but our experiments suggested that KLK10 secreted by TECs is more influential.

We also analyzed molecules that were implicated in cancer cell growth in cooperation with KLK10. The transcriptome analysis by NGS identified 127 genes differentially expressed between TECs and NECs including 58 upregulated genes and 69 downregulated genes. Out of the 58 upregulated genes in TECs, 19 genes have been reported to be associated with cell proliferation, migration, and invasion. For example, Poly (ADP-ribose) polymerase 14 (Parp14) is a gene reported to promote cell proliferation by activation of the NF- κ B pathway in pancreatic cancer,⁴⁰ and heat shock factor 4 (HSF4) is a gene reported to promote cell invasion by enhancing the activity of the c-MET and downstream ERK1/2 and Akt signaling pathways.⁴¹ It is possible that KLK10 may have some interaction with such genes. Moreover, 148 mRNAs showed a more than fourfold difference after KLK10 downregulation, and some of these genes are involved in cell growth based on past literatures. Adenosylmethionine decarboxylase 1 (AMD1) has been reported to enhance cell proliferation, induce cell cycle progression, and inhibit apoptosis.⁴² Dual-specificity phosphatase 1 (DUSP1) has also been reported to inhibit cell proliferation, migration and invasion by blocking the JAK2/STAT3 signaling pathway.⁴³ Based on these results, we considered that KLK10 had an important role in cell proliferation and migration in TEC.

Our data indicate that KLK10 might be a promising therapeutic target for anticancer therapy, but the details of the mechanism of how secreted KLK10 protein might act on TCs remain uncertain. Further studies are needed to clarify whether TCs have receptors for KLK10 or take up KLK10 directly, and how KLK10 affects the cancer microenvironment, including cancer-associated fibroblasts and immune cells. Our group has reported that 6-phosphofructo-2-kinase/fructose-2,6-biphosphatase 3 and glycoprotein nonmetastatic melanoma protein B are upregulated in TECs of mouse HCC models and are associated with tumor vascular normalization and tumor immunity, thereby contributing to tumor proliferation.^{16,27} From the current study and previous reports, we infer that the key molecules in TECs would differ depending on the nature of tumors (hypervascular or hypovascular) and the type of cancer (HCC or CRLM), and that TECs might influence cancer cells via different mechanisms. Several studies have reported that TECs isolated from other malignancies such as renal cancer, lung cancer, melanoma, and HCC show differential patterns of upregulation of molecules.^{17,18,27,39} This variety might suggest that in clinical settings, tumor vascular-targeted therapies should be optimized for each type of malignant tumor.

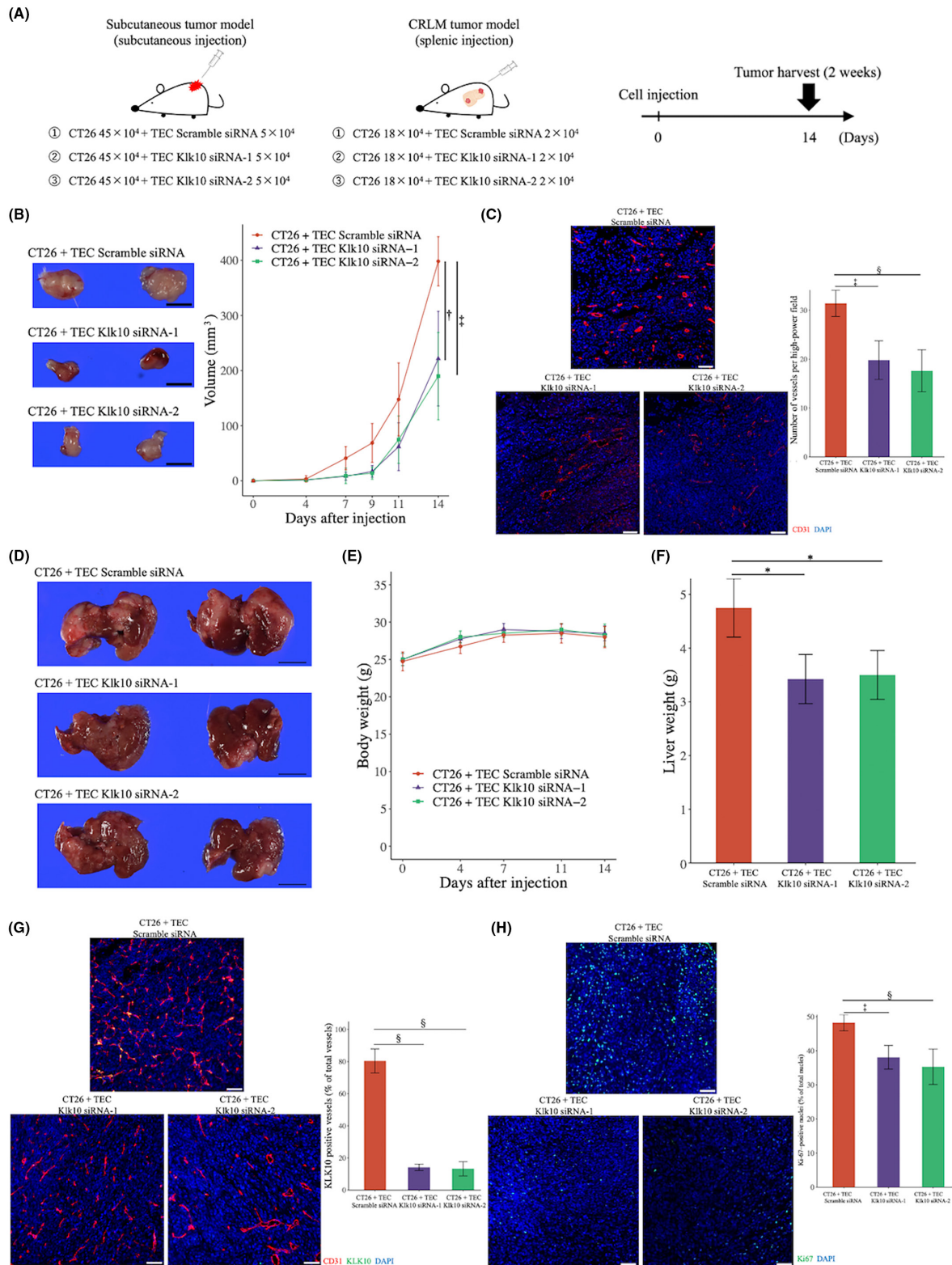


FIGURE 4 The effect of Kik10 downregulation on tumorigenesis in TECs. (A) Schematic illustration of the in vivo experiment: subcutaneous tumor model (left) and CRLM tumor model (right). (B) Subcutaneous tumors and representative pictures (scale bars: 5 mm) and subcutaneous tumor volumes (right). (C) Immunofluorescence images of CD31 staining in subcutaneous tumor (scale bars: 50 μ m) and quantification of vessel numbers (right). (D) CRLM tumors and representative pictures (scale bars: 10 mm). (E) Body weight progress. (F) Comparison of liver weight. (G) Immunofluorescence images of CD31 and Kik10 staining in CRLM tumor (scale bars: 50 μ m). (H) Immunofluorescence images of Ki-67 staining in CRLM tumor (scale bars: 50 μ m) and proportions of Ki-67+ cells among the total number of cells with intact nuclei (right). * $p < 0.05$; † $p < 0.01$; ‡ $p < 0.005$; § $p < 0.001$. CRLM, colorectal liver metastasis; TEC, tumor endothelial cell.

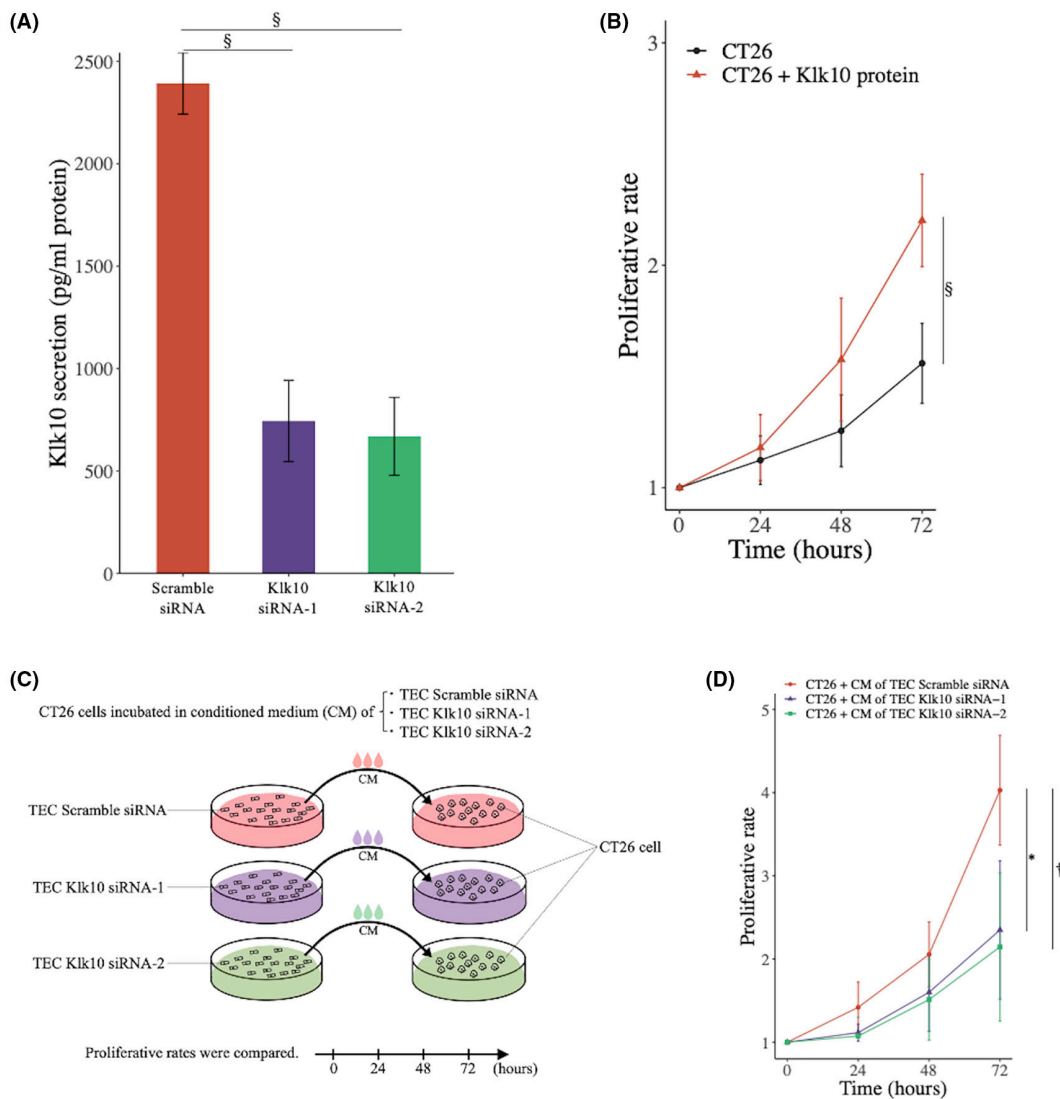


FIGURE 5 Effect of Kik10 in TECs on TC proliferation. (A) Kik10 secretion from TECs with transfected Scramble siRNA, Kik10 siRNA-1, or Kik10 siRNA-2. (B) Effect on CT26 cell proliferation by the addition of Kik10 protein. (C) Schema of the experiment for CT26 cells incubated in CM of transfected TECs. (D) Effect on CT26 cell proliferation by adding CM of transfected TECs. * $p < 0.05$; † $p < 0.01$; § $p < 0.001$. CM, conditioned medium; TC, tumor cell; TEC, tumor endothelial cell.

TABLE 1 Baseline characteristics.

Variables	
Male/female	54/23
Age (years), median (range)	65 (39–85)
BMI (kg/m ²), median (range)	21.6 (16.4–37.3)
Primary tumor T stage, T1/T2/T3/T4	0/10/55/12
Primary tumor N status, -/+	33/44
Primary tumor location, right side/left side	20/57
KRAS, wild-type/mutant-type/unknown	19/14/44
Onset of liver metastasis, synchronous/metachronous	33/44
Number of liver metastases, single/multiple	44/33
Maximum diameter of metastatic lesion (mm), median (range)	25 (5–77)
Distribution of liver metastasis, unilobar/bilobar	54/23
Neoadjuvant chemotherapy before CRLM resection, present/absent	38/39

Abbreviations: BMI, body mass index; CRLM, colorectal liver metastasis; KRAS, V-Ki-ras2 Kirsten rat sarcoma viral oncogene homolog.

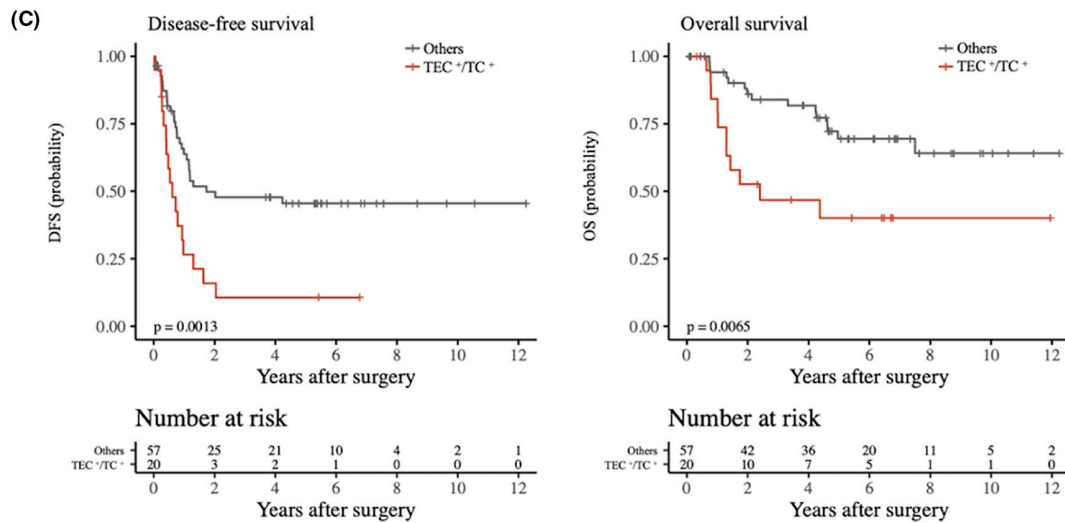
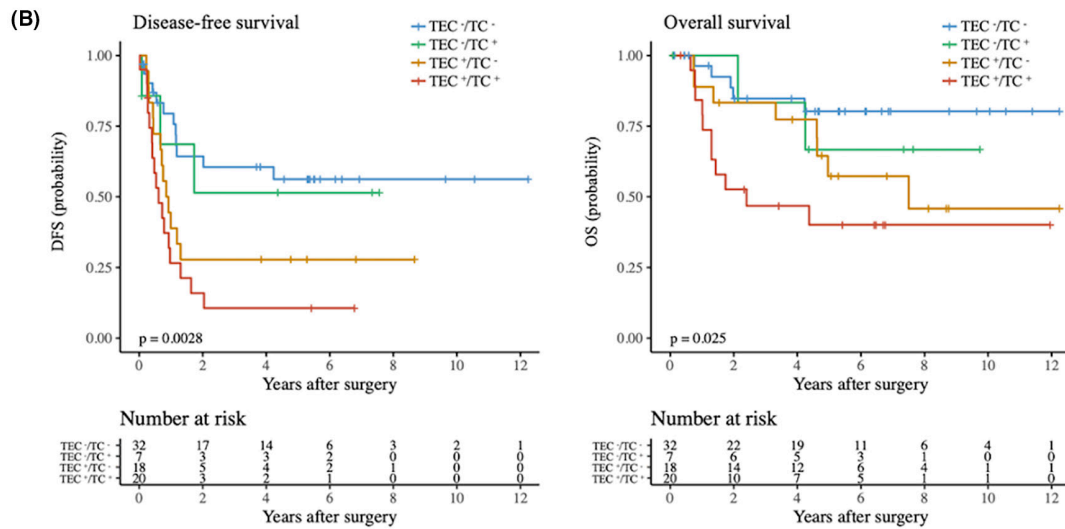
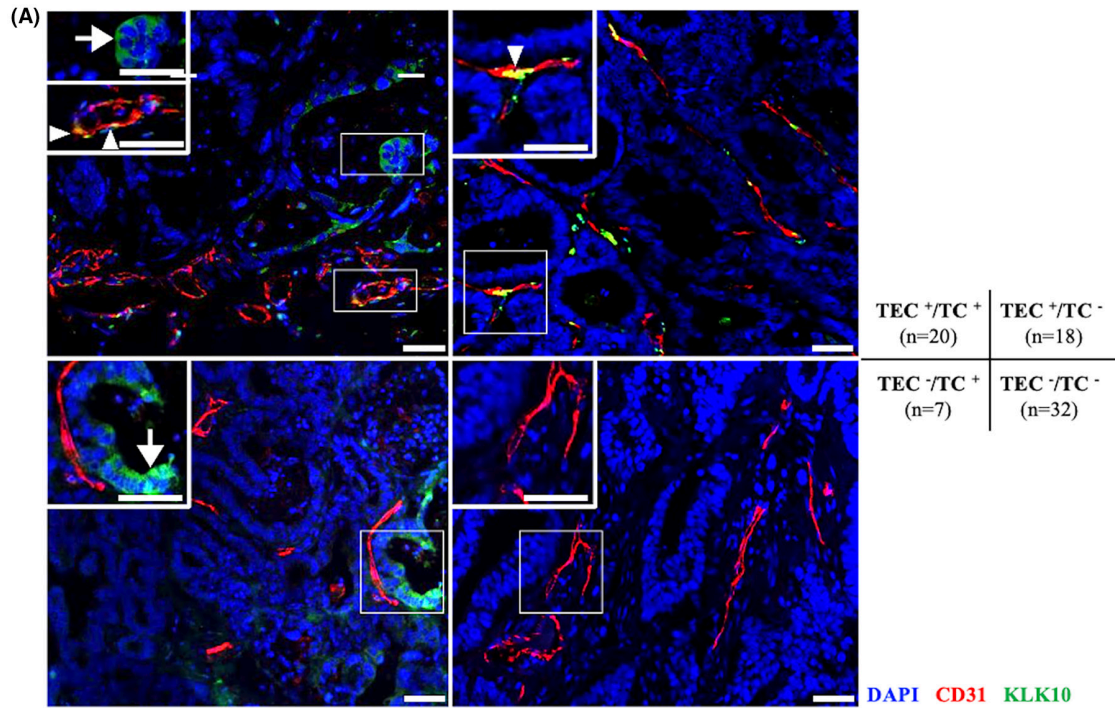


FIGURE 6 Clinical significance of KLK10 expression in TECs and TCs of CRLM. (A) Immunofluorescence analysis demonstrating CD31 and KLK10 expression in CRLM specimens. High-magnification images of the boxed regions are in upper left corner of the merged images. Arrows, KLK10⁺ TCs; arrowheads, KLK10⁺ endothelial cells (scale bar, 50 μm). (B) Kaplan–Meier curves in four groups according to KLK10 expression in TECs and TCs: DFS rates (left) and OS rates (right). (C) Kaplan–Meier curves in two groups of positive KLK10 expression in both TECs and TCs and other patients: DFS rates (left) and OS rates (right). CRLM, colorectal liver metastasis; DFS, disease-free survival; OS, overall survival; TC, tumor cell; TEC, tumor endothelial cell.

TABLE 2 Comparison of clinicopathological features between the TEC⁺/TC⁺ group and the other patients.

Variables	Others	TEC+/TC+	p-Value
	n = 57	n = 20	
Male/female	31/26	7/13	0.218
Age (years), mean ± SD	65 ± 9	63 ± 14	0.456
BMI (kg/m ²), mean ± SD	22.24 ± 3.93	21.58 ± 2.17	0.476
PT (%), mean ± SD	95.5 ± 17.0	100.1 ± 12.5	0.281
Albumin (g/dL), mean ± SD	3.9 ± 0.4	3.7 ± 0.4	0.201
Total bilirubin (mg/dL), mean ± SD	0.8 ± 0.4	0.7 ± 0.3	0.174
CA19-9 (U/mL), mean ± SD	63.9 ± 113.7	98.6 ± 194.1	0.338
CEA (ng/mL), mean ± SD	37.1 ± 87.7	15.8 ± 19.8	0.287
Primary tumor T stage, T2/T3/T4	8/39/10	2/16/2	0.605
Primary tumor N status, -/+	26/31	7/13	0.574
Primary tumor location, right side/left side	15/42	5/15	1
KRAS, wild-type/mutant type/unknown	14/10/33	5/4/11	0.965
Onset of liver metastasis, synchronous/metachronous	21/36	12/8	0.124
Number of liver metastases, single/multiple	33/24	11/9	1
Maximum diameter of metastatic lesion (mm), mean ± SD	30.0 ± 16.5	29.9 ± 17.1	0.985
Distribution of liver metastasis, unilobar/bilobar	40/17	14/6	1
Neoadjuvant chemotherapy before CRLM resection, present/absent	10/47	6/14	0.389

Abbreviations: BMI, body mass index; CA19-9, carbohydrate antigen 19-9; CEA, carcinoembryonic antigen; CRLM, colorectal liver metastasis; KRAS, V-Ki-ras2 Kirsten rat sarcoma viral oncogene homolog; PT, prothrombin time; TC, tumor cell; TEC, tumor endothelial cell.

TABLE 3 Prognostic factors in terms of DFS.

Variables	Univariate		Multivariate	
	Hazard ratio (95% CI)	p-Value	Hazard ratio (95% CI)	p-Value
Male sex	1.25 (0.63–2.46)	0.525	–	–
Age >65 years	0.67 (0.37–1.22)	0.190	–	–
CA19-9 >100 U/mL	4.92 (2.35–10.30)	<0.001	5.09 (2.07–12.51)	<0.001
CEA >10 ng/mL	2.06 (1.14–3.72)	0.016	1.22 (0.62–2.42)	0.561
Primary tumor T stage T3, T4	1.12 (0.45–2.67)	0.786	–	–
Primary tumor N+	2.36 (1.25–4.45)	0.008	1.98 (0.99–3.97)	0.054
Primary tumor location, left side	1.36 (0.69–2.68)	0.379	–	–
Synchronous onset of liver metastasis	2.41 (1.33–4.36)	0.004	1.37 (0.67–2.81)	0.388
Multiple liver metastases	1.91 (1.06–3.45)	0.030	1.09 (0.55–2.19)	0.800
Maximum diameter of liver metastatic lesion >50 mm	1.05 (0.44–2.48)	0.911	–	–
Bilobar distribution of liver metastases	1.60 (0.85–2.98)	0.142	–	–
No neoadjuvant chemotherapy before CRLM resection	0.85 (0.47–1.53)	0.588	–	–
Positive KLK10 expression in TECs and TCs	2.63 (1.43–4.84)	0.002	2.93 (1.49–5.74)	0.002

Abbreviations: CA19-9, carbohydrate antigen 19-9; CEA, carcinoembryonic antigen; CI, confidence interval; CRLM, colorectal liver metastasis; DFS, disease-free survival; KLK10, kallikrein-related peptide 10; TC, tumor cell; TEC, tumor endothelial cell.

TABLE 4 Prognostic factors in terms of OS.

Variables	Univariate		Multivariate	
	Hazard ratio (95% CI)	p-Value	Hazard ratio (95% CI)	p-Value
Male sex	1.31 (0.53–3.27)	0.560	–	–
Age >65 years	1.09 (0.51–2.35)	0.824	–	–
CA19-9 >100U/mL	2.84 (1.13–7.14)	0.027	1.69 (0.63–4.53)	0.296
CEA >10ng/mL	3.23 (1.44–7.27)	0.005	2.39 (1.01–5.69)	0.048
Primary tumor T stage T3, T4	1.29 (0.39–4.31)	0.676	–	–
Primary tumor N+ status	1.67 (0.73–3.85)	0.228	–	–
Primary tumor location, left side	0.93 (0.39–2.21)	0.869	–	–
Synchronous onset of liver metastasis	2.24 (1.02–4.96)	0.046	1.59 (0.69–3.63)	0.274
Multiple liver metastases	1.16 (0.54–2.51)	0.706	–	–
Maximum diameter of liver metastatic lesion >50mm	0.67 (0.20–2.24)	0.517	–	–
Bilobar distribution of liver metastasis	1.32 (0.59–2.97)	0.497	–	–
No neoadjuvant chemotherapy before CRLM resection	1.05 (0.49–2.27)	0.899	–	–
Positive KLK10 expression in TECs and TCs	2.85 (1.30–6.27)	0.009	2.05 (0.91–4.65)	0.084

Abbreviations: CA19-9, carbohydrate antigen 19-9; CEA, carcinoembryonic antigen; CI, confidence interval; CRLM, colorectal liver metastasis; KLK10, kallikrein-related peptide 10; OS, overall survival; TC, tumor cell; TEC, tumor endothelial cell.

In our study of resected specimens, we investigated KLK10 expression in TECs and TCs. Patient samples were divided into four groups based on KLK10 expression status in TECs and TCs, and KLK10 expression in both TECs and TCs was associated with the most unfavorable prognosis. In addition, when compared with the TEC⁻/TC⁺ group, the TEC⁺/TC⁻ group showed a poorer prognosis. These findings suggested that KLK10 expression in TECs contributed more to poor prognosis than KLK10 expression in TCs, which might indicate the importance of KLK10 expression in TECs. These results with clinical specimens are in accordance with the results of our *in vivo* and *in vitro* experiments that KLK10 secreted from TECs could affect colon cancer cell growth acceleration. Moreover, positive KLK10 expression in both TECs and TCs might represent a novel prognostic marker after curative resection of CRLM, and KLK10 in TECs offers a potential therapeutic target for CRLM.

In conclusion, KLK10 derived from TECs would accelerate colon cancer cell proliferation and hematogenous liver metastasis formation. Positive KLK10 expression in both TECs and TCs of CRLM correlated with poor prognosis after curative resection, highlighting KLK10 as a potential prognostic marker and its expression in TECs as a promising therapeutic target in CRLM.

AUTHOR CONTRIBUTIONS

Kazuya Kato: Formal analysis; investigation; methodology; software; visualization; writing – original draft. **Takehiro Noda:** Conceptualization; formal analysis; funding acquisition; methodology; project administration; writing – review and editing. **Shogo Kobayashi:** Resources; supervision; writing – review and editing. **Kazuki Sasaki:** Formal analysis. **Yoshifumi Iwagami:** Formal analysis. **Daisaku Yamada:** Methodology. **Yoshito Tomimaru:** Resources.

Hidenori Takahashi: Resources. **Mamoru Uemura:** Resources. **Tadafumi Asaoka:** Data curation. **Junzo Shimizu:** Data curation. **Yuichiro Doki:** Funding acquisition; supervision. **Hidetoshi Eguchi:** Funding acquisition; supervision.

ACKNOWLEDGMENTS

None.

FUNDING INFORMATION

This work was supported in part by grants from Grant-in-Aid for Scientific Research of the Japan Society for the Promotion of Science ([C] 22K08870) and ([C] 22K16530). The funders had no role in this study.

CONFLICT OF INTEREST STATEMENT

The authors have no conflict of interest.

ETHICS STATEMENT

Approval of the research protocol by an Institutional Reviewer Board: All studies were performed in accordance with the ethical guidelines of the Declaration of Helsinki and Japanese Ethical Guidelines for Human Genome/Gene Analysis Research. The use of resected samples and clinicopathological data was approved by the Human Ethics Review Committee of the Graduate School of Medicine, Osaka University (23126).

Informed Consent: All patients gave written informed consent for research use of their surgical specimens and clinicopathological data, and patient anonymity was preserved.

Registry and the Registration No. of the study/trial: N/A.

Animal Studies: In animal studies, this study was approved by the Animal Experiments Committee, Osaka University (03-085-005).

ORCID

Takehiro Noda  <https://orcid.org/0000-0002-6768-5783>

Shogo Kobayashi  <https://orcid.org/0000-0002-8828-1067>

Daisaku Yamada  <https://orcid.org/0000-0002-6702-3800>

Yoshito Tomimaru  <https://orcid.org/0000-0002-4432-060X>

Hidenori Takahashi  <https://orcid.org/0000-0003-4801-3540>

Hidetoshi Eguchi  <https://orcid.org/0000-0002-2318-1129>

REFERENCES

- Sung H, Ferlay J, Siegel RL, et al. Global cancer statistics 2020: GLOBOCAN estimates of incidence and mortality worldwide for 36 cancers in 185 countries. *CA Cancer J Clin.* 2021;71(3):209-249.
- Holch JW, Demmer M, Lamersdorf C, et al. Pattern and dynamics of distant metastases in metastatic colorectal cancer. *Visc Med.* 2017;33(1):70-75.
- Moreno Prats M, Sasatomi E, Stevenson HL. Colorectal liver metastases: a Pathologist's guide to creating an informative report and improving patient care. *Arch Pathol Lab Med.* 2019;143(2):251-257.
- Tauriello DV, Calon A, Lonardo E, Batlle E. Determinants of metastatic competency in colorectal cancer. *Mol Oncol.* 2017;11(1):97-119.
- Akgul O, Cetinkaya E, Ersoz S, Tez M. Role of surgery in colorectal cancer liver metastases. *World J Gastroenterol.* 2014;20(20):6113-6122.
- de Jong MC, Mayo SC, Pulitano C, et al. Repeat curative intent liver surgery is safe and effective for recurrent colorectal liver metastasis: results from an international multi-institutional analysis. *J Gastrointest Surg.* 2009;13(12):2141-2151.
- Rahbari NN, Birgin E, Bork U, Mehrabi A, Reissfelder C, Weitz J. Anterior approach vs conventional hepatectomy for resection of colorectal liver metastasis: a randomized clinical trial. *JAMA Surg.* 2021;156(1):31-40.
- Folkman J. Role of angiogenesis in tumor growth and metastasis. *Semin Oncol.* 2002;29(6 Suppl 16):15-18.
- Hida K, Kawamoto T, Ohga N, Akiyama K, Hida Y, Shindoh M. Altered angiogenesis in the tumor microenvironment. *Pathol Int.* 2011;61(11):630-637.
- Viallard C, Larrivee B. Tumor angiogenesis and vascular normalization: alternative therapeutic targets. *Angiogenesis.* 2017;20(4):409-426.
- Hida K, Maishi N, Annan DA, Hida Y. Contribution of tumor endothelial cells in cancer progression. *Int J Mol Sci.* 2018;19(5):1272.
- Maishi N, Hida K. Tumor endothelial cells accelerate tumor metastasis. *Cancer Sci.* 2017;108(10):1921-1926.
- Pyaskovskaya ON, Kolesnik DL, Garmanchouk LV, Yanish YV, Solyanik GI. Role of tumor/endothelial cell interactions in tumor growth and metastasis. *Exp Oncol.* 2021;43(2):104-110.
- Fukumura D, Kloepper J, Amoozgar Z, Duda DG, Jain RK. Enhancing cancer immunotherapy using antiangiogenics: opportunities and challenges. *Nat Rev Clin Oncol.* 2018;15(5):325-340.
- Park JS, Kim IK, Han S, et al. Normalization of tumor vessels by Tie2 activation and Ang2 inhibition enhances drug delivery and produces a favorable tumor microenvironment. *Cancer Cell.* 2016;30(6):953-967.
- Matsumoto K, Noda T, Kobayashi S, et al. Inhibition of glycolytic activator PFKFB3 suppresses tumor growth and induces tumor vessel normalization in hepatocellular carcinoma. *Cancer Lett.* 2021;500:29-40.
- Alam MT, Nagao-Kitamoto H, Ohga N, et al. Suprabasin as a novel tumor endothelial cell marker. *Cancer Sci.* 2014;105(12):1533-1540.
- Goveia J, Rohlenova K, Taverna F, et al. An integrated gene expression landscape profiling approach to identify lung tumor endothelial cell heterogeneity and Angiogenic candidates. *Cancer Cell.* 2020;37(1):21-36.e13.
- Saltz LB, Clarke S, Diaz-Rubio E, et al. Bevacizumab in combination with oxaliplatin-based chemotherapy as first-line therapy in metastatic colorectal cancer: a randomized phase III study. *J Clin Oncol.* 2008;26(12):2013-2019.
- Hurwitz H, Fehrenbacher L, Novotny W, et al. Bevacizumab plus irinotecan, fluorouracil, and leucovorin for metastatic colorectal cancer. *N Engl J Med.* 2004;350(23):2335-2342.
- Matsuda K, Ohga N, Hida Y, et al. Isolated tumor endothelial cells maintain specific character during long-term culture. *Biochem Biophys Res Commun.* 2010;394(4):947-954.
- Mukai Y, Yamada D, Eguchi H, et al. Vitamin D supplementation is a promising therapy for pancreatic ductal adenocarcinoma in conjunction with current Chemoradiation therapy. *Ann Surg Oncol.* 2018;25(7):1868-1879.
- Cory G. Scratch-wound assay. *Methods Mol Biol.* 2011;769:25-30.
- Kondo M, Nagano H, Wada H, et al. Combination of IFN-alpha and 5-fluorouracil induces apoptosis through IFN-alpha/beta receptor in human hepatocellular carcinoma cells. *Clin Cancer Res.* 2005;11(3):1277-1286.
- Shinke G, Yamada D, Eguchi H, et al. Role of histone deacetylase 1 in distant metastasis of pancreatic ductal cancer. *Cancer Sci.* 2018;109(8):2520-2531.
- Noda T, Yamamoto H, Takemasa I, et al. PLOD2 induced under hypoxia is a novel prognostic factor for hepatocellular carcinoma after curative resection. *Liver Int.* 2012;32(1):110-118.
- Sakano Y, Noda T, Kobayashi S, et al. Tumor endothelial cell-induced CD8(+) T-cell exhaustion via GPNMB in hepatocellular carcinoma. *Cancer Sci.* 2022;113(5):1625-1638.
- Mikamori M, Yamada D, Eguchi H, et al. MicroRNA-155 controls exosome synthesis and promotes gemcitabine resistance in pancreatic ductal adenocarcinoma. *Sci Rep.* 2017;7:42339.
- Japanese Society for Cancer of the Colon and Rectum. Japanese classification of colorectal, appendiceal, and anal carcinoma: the 3d English edition [secondary publication]. *J Anus Rectum Colon.* 2019;3(4):175-195.
- Cantelmo AR, Conradi LC, Brajic A, et al. Inhibition of the glycolytic activator PFKFB3 in endothelium induces tumor vessel normalization, impairs metastasis, and improves chemotherapy. *Cancer Cell.* 2016;30(6):968-985.
- St Croix B, Rago C, Velculescu V, et al. Genes expressed in human tumor endothelium. *Science.* 2000;289(5482):1197-1202.
- Yousef GM, Diamandis EP. An overview of the kallikrein gene families in humans and other species: emerging candidate tumour markers. *Clin Biochem.* 2003;36(6):443-452.
- Ruckert F, Hennig M, Petraki CD, et al. Co-expression of KLK6 and KLK10 as prognostic factors for survival in pancreatic ductal adenocarcinoma. *Br J Cancer.* 2008;99(9):1484-1492.
- Luo LY, Katsaros D, Scorilas A, et al. The serum concentration of human kallikrein 10 represents a novel biomarker for ovarian cancer diagnosis and prognosis. *Cancer Res.* 2003;63(4):807-811.
- Jiao X, Lu HJ, Zhai MM, et al. Overexpression of kallikrein gene 10 is a biomarker for predicting poor prognosis in gastric cancer. *World J Gastroenterol.* 2013;19(48):9425-9431.
- Wei H, Dong C, Shen Z. Kallikrein-related peptidase (KLK10) cessation blunts colorectal cancer cell growth and glucose metabolism by regulating the PI3K/Akt/mTOR pathway. *Neoplasia.* 2020;67(4):889-897.
- Williams D, Mahmoud M, Liu R, et al. Stable flow-induced expression of KLK10 inhibits endothelial inflammation and atherosclerosis. *elife.* 2022;11:11.
- Butler JM, Kobayashi H, Rafii S. Instructive role of the vascular niche in promoting tumour growth and tissue repair by angiocrine factors. *Nat Rev Cancer.* 2010;10(2):138-146.

39. Maishi N, Ohba Y, Akiyama K, et al. Tumour endothelial cells in high metastatic tumours promote metastasis via epigenetic dysregulation of biglycan. *Sci Rep*. 2016;6:28039.
40. Yao N, Chen Q, Shi W, Tang L, Fu Y. PARP14 promotes the proliferation and gemcitabine chemoresistance of pancreatic cancer cells through activation of NF- κ B pathway. *Mol Carcinog*. 2019;58(7):1291-1302.
41. Zhang W, Zhang X, Cheng P, et al. HSF4 promotes tumor progression of colorectal cancer by transactivating c-MET. *Mol Cell Biochem*. 2023;478(5):1141-1150.
42. Gao H, Li H, Wang J, et al. Polyamine synthesis enzyme AMD1 is closely related to the tumorigenesis and prognosis of human breast cancer. *Exp Cell Res*. 2022;417(2):113235.
43. Chen H, Ren S, Wan H, Wei W, Luo Y, Cai M. DUSP1 regulates the JAK2/STAT3 signaling pathway through targeting miR-21 in cervical cancer cells. *Cell Mol Biol (Noisy-le-Grand)*. 2023;69(8):40-44.

SUPPORTING INFORMATION

Additional supporting information can be found online in the Supporting Information section at the end of this article.

How to cite this article: Kato K, Noda T, Kobayashi S, et al. KLK10 derived from tumor endothelial cells accelerates colon cancer cell proliferation and hematogenous liver metastasis formation. *Cancer Sci*. 2024;115:1520-1535. doi:[10.1111/cas.16144](https://doi.org/10.1111/cas.16144)